

# Rab4 Regulates Formation of Synaptic-like Microvesicles from Early Endosomes in PC12 Cells

Heidi de Wit,\* Yael Lichtenstein,<sup>†</sup> Regis B. Kelly,<sup>†</sup> Hans J. Geuze,\* Judith Klumperman,<sup>‡§||</sup> and Peter van der Sluijs<sup>§||¶</sup>

<sup>¶</sup>Department of Cell Biology and Institute of Biomembranes, University Medical Center, 3584 CX Utrecht, The Netherlands and <sup>‡</sup>Center for Biomedical Genetics, The Netherlands; and <sup>†</sup>Department of Biochemistry and Biophysics, Hormone Research Institute, University of California, San Francisco, California 94143-0534

Submitted February 2, 2001; Revised August 24, 2001; Accepted August 31, 2001  
Monitoring Editor: Vivek Malhotra

Early endosomes in PC12 cells are an important site for the formation of synaptic-like microvesicles and constitutive recycling vesicles. By immunogold electron microscopy, the small GTPase rab4 was localized to early endosomes and numerous small vesicles in the cell periphery and Golgi area of PC12 cells. Overexpression of GTPase-deficient Q67Lrab4 increased the number of early endosome-associated and cytoplasmic vesicles, whereas expression of GDP-bound S22Nrab4 significantly increased the length of early endosomal tubules. In parallel, Q67Lrab4 induced a shift in rab4, VAMP2, and TfR label from early endosomes to peripheral vesicles, whereas S22Nrab4 increased early endosome labeling of all three proteins. These observations were corroborated by early endosome budding assays. Together, our data document a thus far unrecognized role for rab4 in the formation of synaptic-like microvesicles and add to our understanding of the formation of constitutive recycling vesicles from early endosomes.

## INTRODUCTION

Neurons contain synaptic vesicles (SVs) that release neurotransmitters by fusion with the presynaptic zone in response to elevated levels of intracellular calcium. After exocytosis, SV membrane proteins are internalized to be reutilized in locally reformed SVs (Hannah *et al.*, 1999). This cycle of exocytosis and endocytosis is unique with respect to its high speed and allows the presynaptic neuron to maintain high rates of neurotransmitter release. Neuroendocrine cells lack synaptic specializations, but also produce neurotransmitter-containing vesicles that are named synaptic-like microvesicles (SLMVs). Cell free assays and electron microscopic (EM) studies have shown that SLMVs are reformed at two distinct locations in the cell; the plasma membrane (Schmidt *et al.*, 1997; Shi *et al.*, 1998) and early endosomes (EEs; Lichtenstein *et al.*, 1998; de Wit *et al.*, 1999). An additional layer of complexity is added by the observations that distinct SLMV proteins are targeted predominantly from

either the plasma membrane or from EEs to SLMVs, as was shown for synaptotagmin (Blagoveshchenskaya *et al.*, 1999) and VAMP2 (Shi *et al.*, 1998), respectively. Formation of SLMVs at the two different locations occurs by biochemically distinct mechanisms. In vitro assays reconstituting SLMV formation in neuroendocrine PC12 cells showed that clathrin, the AP-2 adaptor complex, dynamin, and endophilin are required at the plasma membrane (Shi *et al.*, 1998; Schmidt *et al.*, 1999). In contrast, SLMV budding from EEs occurs independently of clathrin, but requires the AP-3 adaptor complex and depends on the presence of the small GTPase ARF1 (Faúndez *et al.*, 1997, 1998). In either case, SV membrane proteins such as VAMP2 (synaptobrevin 2) and synaptotagmin, have to be sorted from non-SV proteins such as transferrin receptor (TfR). The mechanisms by which SV proteins are sorted from non-SV proteins are largely unknown. Because the ear-domains of the large adaptin subunits constitute interaction sites for many accessory proteins involved in endocytosis (Owen *et al.*, 1999; Page *et al.*, 1999), most likely additional, yet unknown proteins will be found regulating formation of SVs.

The two small GTPases rab5 and rab4 regulate transport to and through EEs, respectively (Bucci *et al.*, 1992; van der Sluijs *et al.*, 1992). Rab5 is required for fusion of primary endocytic vesicles with EEs in vivo, as well as homotypic EE fusion in vitro (Gorvel *et al.*, 1991). Several lines of evidence show that rab4 regulates the exit of constitutive recycling

\* Corresponding authors. E-mail addresses: pvander@knoware.nl or j.klumperman@lab.azu.nl.

<sup>§</sup>J.K. and P.vdS. contributed equally to this work.  
Abbreviations used: SV, synaptic vesicle; SLMV, synaptic-like microvesicle; EM, electron microscopy; EE, early endosome; TfR, transferrin receptor; TGN, *trans*-Golgi network; CD-MPR, cation-dependent mannose-6 phosphate receptor; VAMP, vesicle-associated membrane protein.

cargo from EEs in nonneuronal cells (van der Sluijs *et al.*, 1992). Overexpression of rab4 causes a redistribution of TfR from EEs to the plasma membrane. Furthermore, iron discharge from internalized transferrin is reduced in these cells because of accumulation of transferrin in nonacidic vesicles and tubules, also known as perinuclear recycling endosomes. These Tf-positive vesicles and tubules are enriched in cellubrevin and Tf, but are relatively depleted of rab4 and enriched in rab11 (Daro *et al.*, 1996; Sheff *et al.*, 1999; Sönrichsen *et al.*, 2000). Thus, rab4 likely acts to transfer EE-derived transport vesicles to recycling endosomes. In addition to a function in constitutive recycling of TfR, rab4 also controls more specific transport steps. In fat and muscle cells, rab4 regulates translocation of the insulin-responsive glucose transporter GLUT4 from an intracellular storage compartment to the plasma membrane (Shibata *et al.*, 1996; Vollenweider *et al.*, 1997). Both translocation of GLUT4 and recycling of SV proteins are tightly regulated to maintain a readily releasable pool of intracellular vesicles that is accessible to endocytosed tracers. This parallel between the translocation of GLUT4 containing transport vesicles and recycling of SVs might indicate a possible involvement of rab4 in SV recycling from EEs. Although rab4 cDNA was initially cloned from a brain cDNA library (Zahraoui *et al.*, 1989), neither the rab4 subcellular distribution nor its functional importance have been analyzed in neuronal cell types.

The pheochromocytoma cell line PC12 is a useful experimental system to investigate the formation of SVs, because it contains SLMVs that share many properties with neuronal SVs (Clift-O'Grady *et al.*, 1990; Cameron *et al.*, 1991; Linstedt and Kelly, 1991; Bauerfeind *et al.*, 1993; Blagoveshchenskaya and Cutler, 2000). Our previous ultrastructural studies in PC12 cells showed that EEs are precursors of SLMVs and contain rab4 (de Wit *et al.*, 1999). In the present study we investigated a possible role of rab4 in SLMV formation. Our morphological and biochemical data show that rab4 regulates budding of SLMVs and constitutive recycling vesicles from EEs.

## MATERIALS AND METHODS

### Antibodies and Reagents

Rabbit antisera against rab4 (Bottger *et al.*, 1996), cation-dependent mannose 6-phosphate receptor (CD-MPR; Klumperman *et al.*, 1993), and the mouse monoclonal antibodies against VAMP2 (Cl 69.1; Edelmann *et al.*, 1995), synaptotagmin (Cl 604.1), and human TfR (H68.4; White *et al.*, 1992) were described previously. These antibodies recognize cytosolically exposed epitopes, except Cl 604.1, which binds luminal epitopes of synaptotagmin. A bridging rabbit anti-mouse IgG antibody (DAKO, Glostrup, Denmark) was used to provide binding sites for protein A-gold, when sections were labeled with mouse monoclonal antibodies. Tf-HRP was purchased from Jackson Immunoresearch Laboratories (West Grove, PA) and was iron saturated as previously described (Lichtenstein *et al.*, 1998).

### Cell Culture and Transfection

The 251-II PC12 clone was generously provided by Wieland Huttner (University of Heidelberg, Germany) and grown under conditions in which the cells have an endocrine phenotype and do not form neurites (de Wit *et al.*, 1999). cDNAs encoding wild-type rab4, Q67Lrab4, or S22Nrab4 were subcloned in the *EcoRI* site of the mammalian expression plasmid pcDNA3 (Invitrogen, Leek, The Netherlands). Cells from a confluent 15-cm dish were resuspended

in 650  $\mu$ l electroporation buffer (137 mM NaCl, 5 mM KCl, 0.7 mM  $\text{Na}_2\text{HPO}_4$ , 6 mM glucose, 20 mM HEPES, pH 7.05) together with 60  $\mu$ g DNA and electroporated at 500  $\mu$ F and 230 mV. Cells were transferred to 20 ml of culture medium supplemented with 3 mM EGTA and allowed to recover for 30 min at 37°C. Next, the cells were harvested at 800  $\times$  g for 5 min and plated on two 10-cm dishes. After 2 d, the cells were transferred to media containing 450  $\mu$ g/ml G418. Stable transfectants were screened by immunofluorescence microscopy. Western blot analysis showed that the rab4 cDNA products were expressed to the same level in wild-type rab4, rab4Q67L, and rab4S22N transfectants. Expression in these cell lines was  $\sim$ 10-fold above endogenous rab4. Cells received 5 mM sodium butyrate 18–24 h before all experiments to induce expression of the CMV-driven cDNA products.

### Immunogold Electron Microscopy

PC12 cells were prepared for ultrathin cryosectioning and (double-)immunogold labeled as described (Slot *et al.*, 1991; de Wit *et al.*, 1999). Semiquantitative analysis of rab4, TfR, VAMP2, and CD-MPR distributions was carried out as follows. Cryosections with good ultrastructure were selected at low magnification and scanned at 20,000 $\times$  magnification along a fixed track. All gold particles within a distance of 30 nm from a membrane were assigned to that organelle and at least two independent quantitations were performed for each protein. In total, at least 1200 gold particles for each protein were counted. The distribution of gold particles was expressed as the percentage of total gold particles that was found over a specific compartment. Endosomal compartments were defined as previously described (de Wit *et al.*, 1999). Forty-nanometer tubulo-vesicular profiles were included in the category "EEs" when they were at a distance of no more than 100 nm from an endosomal vacuole. All other 40-nm tubulo-vesicles were, according to their location, assigned to the Golgi region or described as peripheral vesicles. TfR and VAMP2 in addition to EEs and small vesicles also labeled other compartments, such as Golgi, plasma membrane, and specifically VAMP2 secretory granules. However, because label over these compartments was not significantly different between the two mutant rab4-expressing cell lines, for reason of clarity these compartments were not incorporated in Table 3. Instead, the number of gold particles found over EEs and cytoplasmic vesicles was set to 100%.

To determine the membrane length of vacuolar and tubular EEs (see Table 2), 30 pictures were taken at 30,000 $\times$  magnification of rab4-labeled sections prepared from control cells and rab4 transfectants. A transparency displaying a squared lattice of lines that were 0.5  $\mu$ m apart was put over the pictures and analyzed for intersections with the membranes of interest. The number of intersections was taken as a measure for membrane length (Staubli *et al.*, 1969; Weibel *et al.*, 1969). For EE tubules, only those membrane profiles of which the length was at least twice that of the diameter and that were connected to an EE vacuole were taken into account. Membrane profiles within 100 nm of an EE vacuole of which the length was less than twice the diameter and that showed no continuities with the vacuole were designated as EE vesicles. The degree of colocalization of rab4 with VAMP2 and TfR was analyzed in double-labeled sections. Thirty cell profiles were screened of Q67Lrab4 and S22Nrab4 transfectants, respectively, and all vesicles encountered were analyzed for the presence of rab4 and VAMP2 or TfR. Statistical comparisons were done with the Student's *t* test.

### Internalization of $^{125}\text{I}$ -Cl604.1 and In Vivo SLMV Budding Assay

Cl604.1 was iodinated as described (Lichtenstein *et al.*, 1998). Confluent 15-cm tissue culture dishes were rinsed three times with labeling buffer (Clift-O'Grady *et al.*, 1998). Cells were preincubated for 15 min on ice with 5  $\mu$ g/ml  $^{125}\text{I}$ -Cl604.1. After 15 min the labeled antibody was aspirated, and bound  $^{125}\text{I}$ -Cl604.1 was chased into EEs during an incubation for 40 min at 15°C. The cells were then washed

three times with ice-cold uptake buffer, incubated for 15 min at 37°C and homogenized as described (Clift-O'Grady *et al.*, 1998). Homogenates were centrifuged at  $1000 \times g$  for 5 min to prepare a postnuclear supernatant (Lichtenstein *et al.*, 1998). Postnuclear supernatants were next centrifuged at  $27,000 \times g$  for 35 min. The SLMVs in this supernatant were resolved on 5–25% glycerol velocity gradients and spun for 75 min at  $218,000 \times g$  in a SW55 rotor. Fractions were collected from the bottom and  $^{125}\text{I}$ -Cl604.1 was detected in a  $\gamma$ -counter.

### ***Tf*-HRP Internalization and In Vitro EE Budding Assay**

Cells grown on 15-cm dishes were incubated 1 h at 37°C in serum-free medium to deplete endogenous Tf. Iron saturated rat Tf-HRP (20  $\mu\text{g}/\text{ml}$ ) was endocytosed for 40 min at 15°C. Cell surface-bound Tf-HRP was removed during two washes with ice-cold PBS, 0.3 mM  $\text{CaCl}_2$ , 0.3 mM  $\text{MgCl}_2$ , 1 mg/ml glucose, and 3% protease-free BSA (labeling buffer; Clift-O'Grady *et al.*, 1998) and centrifuged at  $800 \times g$  for 5 min. The cells were collected in 25 ml 38 mM K-aspartate, 38 mM K-glutamate, 38 mM K-gluconate, 5 mM reduced glutathione, 5 mM Na-carbonate, 2.5 mM Mg-sulfonate, 20 mM K-MOPS, pH 7.2 (bud buffer), and pelleted at  $800 \times g$  for 5 min. This wash was repeated once, and the cells were homogenized in bud buffer containing protease inhibitors as previously described (Clift-O'Grady *et al.*, 1998). A postnuclear supernatant was prepared by spinning the homogenates for 5 min at  $1000 \times g$ , and 1-mg aliquots were used as a donor fraction for the in vitro budding of transport vesicles containing Tf-HRP. The donor fraction was incubated for 30 min at 37°C or at 0°C (control) in the presence of 1 mM ATP, 8 mM creatine phosphate, 5  $\mu\text{g}/\text{ml}$  creatine kinase, and 3 mg/ml rat brain cytosol (Desnos *et al.*, 1995). To resolve newly formed vesicles from the donor compartment, budding reactions were layered on top of a 10–45% sucrose gradient buffered with 20 mM K-MOPS, pH 7.2, and centrifuged for 1 h at  $116,000 \times g$  in a SW 55 rotor. Fractions were collected from the bottom and Tf-HRP in gradient fractions was assayed colorimetrically as described (Lichtenstein *et al.*, 1998).

## **RESULTS**

Thus far, the localization of rab proteins has been done mainly at the light microscopic level. However, to fully understand the function of rab proteins in determining specific transport pathways, it is a prerequisite to establish their precise intracellular localization. We here set out to define the subcellular localization of rab4 by immuno-EM in the morphologically well-characterized PC12 neuroendocrine cells (de Wit *et al.*, 1999). We studied endogenous rab4 as well as stable PC12 cell transfectants expressing wild-type rab4, a GTP-hydrolysis deficient mutant (Q67Lrab4 cells), or a GDP-bound form of rab4 (S22Nrab4 cells).

### ***Ultrastructural Localization of rab4***

By immunogold labeling of ultrathin cryosections of PC12 cells, we found that endogenous rab4 mainly associated with EEs and small cytoplasmic vesicles (Figure 1, A and B; Table 1). EEs in PC12 cells have been well defined, and consist of two subdomains: i) heterogeneously sized electron-lucent vacuoles with few internal vesicles, and ii) numerous  $\sim 40$ -nm tubules, which mediate recycling from EEs to the *trans*-Golgi network (TGN) and plasma membrane (Geuze *et al.*, 1984; Marsh *et al.*, 1986; Klumperman *et al.*, 1993; de Wit *et al.*, 1999). In ultrathin cryosections, EE recycling tubules appear as tubulo-vesicular profiles with, in the plane of the section, only occasional continuities with the EE vacuole. Rab4 was found on both the vacuolar and tubular

EE subdomains (Figure 1, A and C). To standardize our quantitative studies, we included the endosomal vacuole plus all tubulo-vesicular membrane profiles at no more than 100 nm distance in our definition of the category EEs. Of the non-EE-associated rab4-positive vesicles  $\sim 40\%$  was found in the *trans*-Golgi region, that is, at a magnification of  $20,000\times$  in the same EM image as and at the *trans*-side of the Golgi stack (Figure 1B). The others were found in the cell periphery, where they sometimes formed small clusters (see e.g., Figure 1C). Cells stably overexpressing rab4 (wild-type rab4 cells) showed labeling densities that were significantly (5–10 times) higher than those in nontransfected control cells, but with a very similar if not identical distribution as endogenous rab4 (Figure 1C; Table 1). The plasma membrane was invariably devoid of rab4 (Figure 1, A and C), consistent with earlier findings that showed that rab4 is not involved in internalization from the cell surface (van der Sluijs *et al.*, 1992). Unexpectedly, a small number of rab4-representing gold particles ( $\sim 5\%$ ) was present over the Golgi stack. This labeling proportionally increased upon rab4 overexpression and occurred both in the wild-type and mutant rab4-expressing cells. The implication of this observation as yet remains unclear. Rab4 was absent from late endosomes and lysosomes as previously defined (de Wit *et al.*, 1999) and secretory granules (Figure 1, B and C). The absence of rab4 from late endocytic compartments extends the notion that rab4 regulates recycling from EEs rather than transport events in the late endosome-lysosome pathway.

### ***Overexpression of Wild-type rab4 Increases the Length of EE Recycling Tubules***

On transfection of wild-type rab4 cDNA in PC12 cells, we observed a striking increase in membrane-length of the EE-associated tubules, which was accompanied by a significant decrease in membrane length of the vacuolar portion of EEs (Table 2). Nontransfected PC12 cells treated with butyrate did not yield this phenotype (our unpublished results). Thus, although rab5 overexpression produces enlarged EE vacuoles (Bucci *et al.*, 1992), moderate overexpression of rab4 induces an opposite effect, resulting in an increase in the length of the endosomal recycling tubules.

### ***Rab4 Mutants Have Distinct Localizations and Opposite Morphological Phenotypes***

To define the distribution patterns of activating and inhibitory rab4 mutants and to investigate their effect on EE morphology, we stably transfected PC12 cells with Q67Lrab4 and S22Nrab4. In Q67Lrab4 cells we found a shift in the distribution of rab4 to the small cytoplasmic vesicles (especially those located at the periphery), at the expense of EEs (Figure 2, A and B; Table 1). Because labeling densities of single vesicles were alike in wild-type rab4 and Q67Lrab4 cells, this finding indicates an increase in the number of rab4-positive peripheral vesicles in the latter. Notably, the EE tubules in Q67Lrab4 cells were substantially shorter than those in wild-type rab4 cells, whereas more EE-associated vesicles were present (Table 2). In S22Nrab4 cells, the EE tubules were markedly elongated and significantly longer than the already enlarged tubules in wild-type rab4 cells (Figure 2C; Table 2).

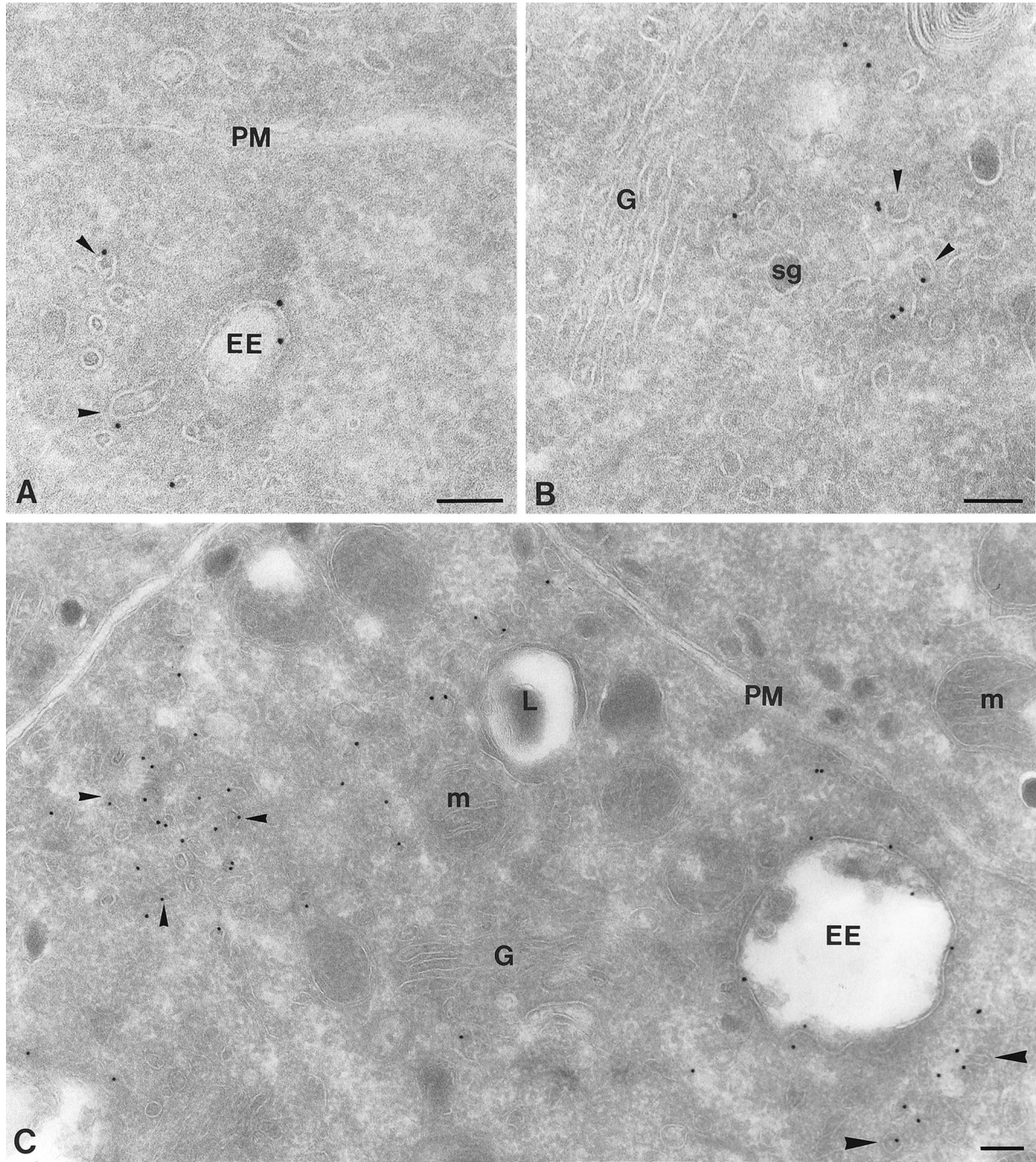


**Figure 1.** Ultrathin cryosections of PC12 cells showing immunogold labeling for endogenous rab4 (A and B) and overexpressed rab4 (C). (A) Endogenous rab4 is present on EE vacuoles (EE) and nearby located vesicles and tubules (arrowheads), whereas the plasma membrane (PM) is devoid of label. (B) Rab4-positive vesicles (arrowheads) are also present at the *trans*-side of the Golgi (G). (C) In rab4 overexpressing cells, a similar labeling pattern is seen as for endogenous rab4, but with significantly increased density. The small arrowheads point to a cluster of rab4-positive vesicles in the peripheral cytoplasm. The large arrowheads point to vesicles more closely located near an EE. M, mitochondrion; SG, secretory granule; L, lysosome. Bars, 100 nm.

The number of vesicular profiles around EEs was largely reduced in these cells. Furthermore, the GDP-bound mutant S22Nrab4 was prominently present on EEs and to a

lesser extent on small vesicles (Figure 2, C and D; Table 1). Thus, in comparison to wild-type rab4, expression of the GTP-bound mutant Q67L resulted in a decrease of endo-

**Table 1.** Subcellular distribution of endogenous and stably expressed wild-type rab4, Q67Lrab4, and S22Nrab4

	Golgi stacks	EEs	Vesicles	
			Golgi area	Peripheral cytoplasm
Endogenous rab4	6 ± 0.8	36 ± 2.7	25 ± 2.6	33 ± 2.9
Wild-type rab4	4 ± 1.4	40 ± 2.1	22 ± 1.2	34 ± 1.0
Q67Lrab4	6 ± 1.5	27 ± 3.2	25 ± 3.2	42 ± 2.1
S22Nrab4	5 ± 1.2	48 ± 4.9	15 ± 2.6	32 ± 2.5

Data represent the average percentages ± SEM of the total number of gold particles that were found over the indicated compartments. EEs, vacuole plus associated tubulo-vesicles.

somal labeling and an increase in the number of rab4-positive vesicles, whereas the GDP-bound mutant S22N resulted in the opposite effect. In addition, the average length of EE recycling tubules was significantly increased in S22Nrab4 cells. Together, these data suggest that rab4-GTP stimulates vesicle formation from EE tubules, resulting in a decreased average tubule length.

#### **Rab4 Mutants Differentially Affect SLMV Formation**

In a previous study we have described that SLMVs are formed from EE tubules (de Wit *et al.*, 1999). Our finding that rab4 affects vesicle formation from EE tubules therefore motivated us to study whether rab4 could be involved in SLMV formation. Because the effects on EE-derived tubule and vesicle formation were most prominent in the S22N and Q67Lrab4 cells, we focused on these two cell lines for further studies. As a marker for SLMVs, we used VAMP2/synaptobrevin2. In Q67Lrab4 cells, 90% of the total EE and vesicle-associated VAMP2 was found in small vesicles that were distributed in the Golgi area and peripheral cytoplasm (Table 3; Figure 3, A and B). In a previous study in PC12 cells we have shown that these VAMP2-positive vesicles contain additional SLMV marker proteins such as synaptophysin and rab3 but are depleted in TfR, indicating that they largely represent SLMVs (de Wit *et al.*, 1999). In S22Nrab4 PC12 transfectants, a much larger portion (57%) of VAMP2 was associated with EEs, and only 43% with SLMVs, of which only few were found in the Golgi area (Figure 3, C and D;

Table 3). These shifts in the relative distributions of VAMP2 over EEs and SLMVs in the two mutants paralleled that of rab4 itself. To establish whether rab4 might have a direct effect on VAMP2 trafficking, we performed double-immunogold labeling. This indeed showed colocalization of VAMP2 and rab4 in small vesicles (Figure 3), which represent SLMVs (de Wit *et al.*, 1999). The extent of this colocalization did not alter when the two different rab4 mutants were expressed. In both cell lines, of all vesicles labeled for rab4, VAMP2, or both, 23% were found positive for both rab4 and VAMP2.

#### **Rab4 Mutants Differentially Affect the Localization of TfR**

EEs also mediate the constitutive recycling of TfR, which is sorted to different tubular extensions than recycling SLMV proteins (de Wit *et al.*, 1999). In nonneuroendocrine cells a regulatory role of rab4 in TfR recycling has been suggested (van der Sluijs *et al.*, 1992; Chavrier *et al.*, 1997), which prompted us to investigate the role of rab4 in TfR recycling in PC12 cells. Like rab4 and VAMP2, TfR-positive recycling vesicles were found both in the Golgi region and in the peripheral cytoplasm. Furthermore, similar to the redistribution of rab4 itself, expression of Q67Lrab4 in PC12 cells caused a shift in TfR distribution from EEs to recycling vesicles, whereas S22Nrab4 increased endosomal labeling of TfR (Table 3). To investigate whether rab4 was indeed

**Table 2.** Morphological changes in EEs after transfection of PC12 cells with wild type rab4, Q67Lrab4, and S22Nrab4

	No. of EE-associated vesicles	Membrane length (nm)	
		EE vacuole	EE tubules
Endogenous rab4	6.8 ± 0.6	1410 ± 38	142 ± 23
Wild-type rab4	9.1 ± 0.7	618 ± 27	379 ± 45
Q67Lrab4	13.5 ± 1.0	619 ± 28	181 ± 19
S22Nrab4	4.4 ± 0.6	940 ± 36	508 ± 37

The average number of vesicles (± SEM) associated with an EE was determined by counting all vesicular profiles within 100 nm of an EE vacuole of which the length was less than twice the diameter. The average membrane length ± SEM of EE vacuoles and tubules was established by counting the number of intersections with a lattice overlay. Only tubules that were visibly connected to the EE vacuolar domain were taken into account. Countings were done on 30 EEs (defined as in de Wit *et al.*, 1999) of each cell line.

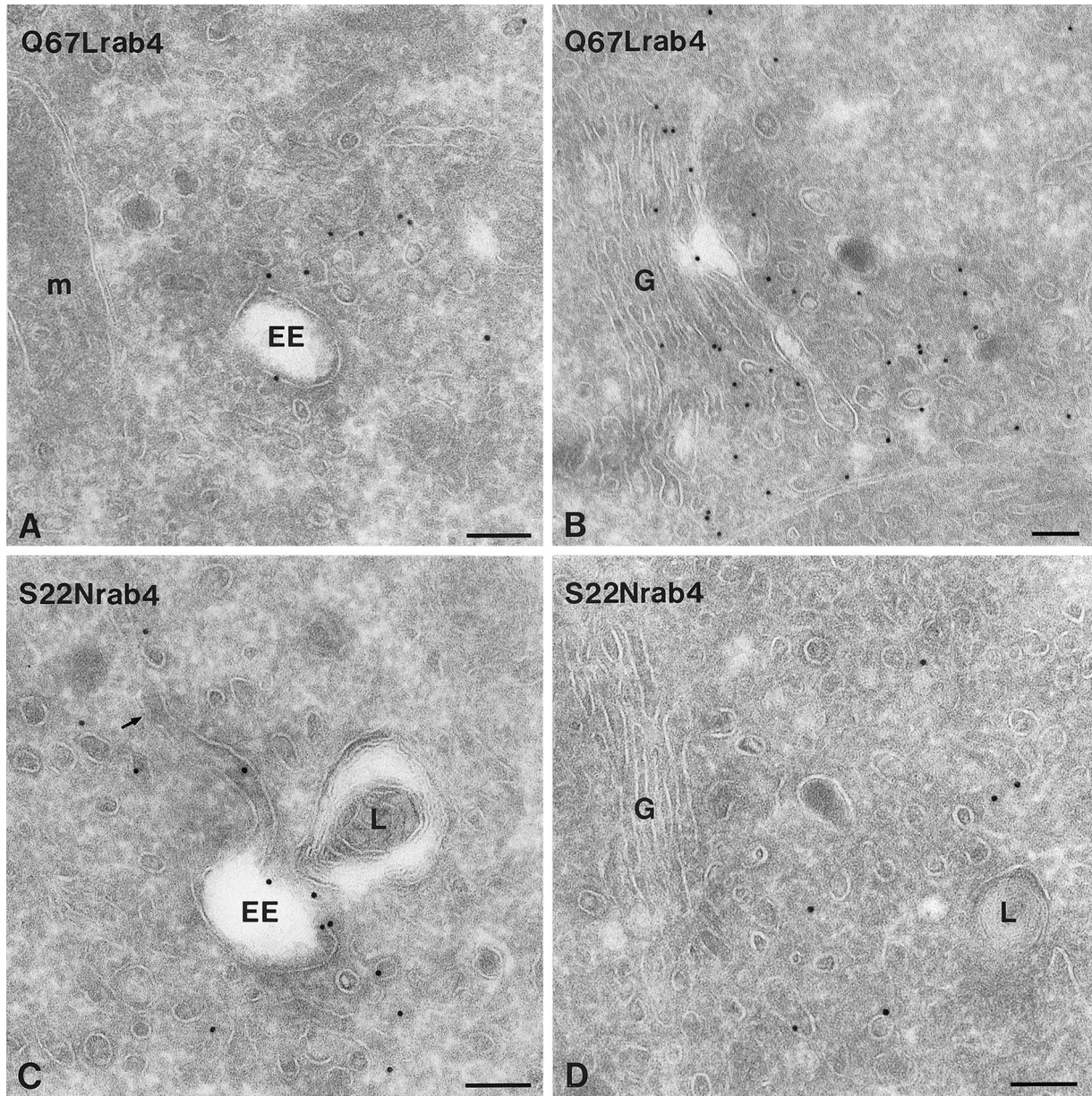


**Figure 2.** Ultrathin cryosections of PC12 cells expressing rab4 mutants as indicated on the pictures. (A) Low amounts of Q67Lrab4 are present on early endosomes (EE) and associated vesicles. (B) In contrast, Q67Lrab4 labels many small vesicles at the *trans*-side of the Golgi stack (G). (C) An opposite distribution pattern was found for S22Nrab4. S22Nrab4 was frequently associated with EE vacuoles and associated vesicles and tubules. The arrow points to an EE tubule, which are significantly extended in S22Nrab4 cells. (D) S22Nrab4 labeled only few vesicles in the Golgi area. L, lysosome; M, mitochondrion. Bars, 100 nm.

present on vesicles mediating transport of TfR we performed double-immunogold labeling (Figure 4, A and B). We found that in both Q67L and S22Nrab4 cells 15% of all labeled vesicles contained rab4 as well as TfR. As a control for our quantitative measurements we established the distribution of the cation-dependent mannose 6-phosphate receptor (CD-MPR). This receptor cycles between the TGN and endosomes and does not colocalize with rab4 (Klumperman *et al.*, 1993). CD-MPR was mainly localized to the

TGN (our unpublished results) and its distribution was similar in the two mutant rab4 cell lines, indicating that the effects of rab4 expression on the redistribution of VAMP2 and TfR are specific. To investigate whether rab4 affected the comparative distribution of the two cargo molecules, we performed a double-labeling with antibodies against TfR and VAMP2 on sections prepared from S22Nrab4 cells. We chose this cell line because the mutant accumulated the marker proteins in EE-associated tubules. We reasoned that

**Table 3.** Redistribution of TfR and VAMP-2 in rab4 mutant cell lines

	EEs	Vesicles	
		Golgi area	Peripheral vesicles
VAMP-2			
Q67Lrab4	10 ± 1.9	42 ± 2.4	48 ± 2.8
S22Nrab4	57 ± 4.9	13 ± 1.2	30 ± 2.5
TfR			
Q67Lrab4	16 ± 1.8	44 ± 1.8	40 ± 3.7
S22Nrab4	51 ± 2.9	26 ± 1.9	23 ± 2.0

Data represent the percentages ± SEM of total gold found over the indicated compartments. EEs, vacuole plus associated tubulo-vesicles.

if rab4 had any effect on the segregation of the two proteins, this should be an early event taking place in EE, and not during or after the formation of transport vesicles. As shown in Figure 5, VAMP2 and TfR colocalized to the vacuolar portion of the same EE, whereas most of the EE-associated tubulovesicles contained either VAMP2 or TfR. We previously reported similar findings in control PC12 cells (Lichtenstein *et al.*, 1998; de Wit *et al.*, 1999); thus, rab4 appeared to act after the two molecules are sorted away from each other. Taken together, the immuno-EM data showed that the two distinct endocytic recycling pathways taken by VAMP2 and TfR are regulated in a similar manner by rab4. The active form of rab4 caused a redistribution of the regulated recycling marker VAMP2 as well as the constitutively recycling protein TfR to vesicles adjacent to the Golgi complex and the peripheral cytoplasm, whereas the GDP-bound rab4 mutant caused a redistribution of both proteins to EE-associated vesicles and tubules. Thus, rab4-GTP appears to regulate the exit of constitutive and regulated recycling proteins from EEs.

#### Rab4 Controls Budding of Synaptic-like Microvesicles from EEs

To confirm by an independent approach that rab4 regulates SLMV recycling, we used a biochemical assay that reproduces SLMV formation from EEs in PC12 cells (Clift-O'Grady *et al.*, 1998). First,  $^{125}\text{I}$ -Cl 604.1 mAb against a luminal epitope of the SLMV marker synaptotagmin was added to cells kept at 15°C, which results in its accumulation in EEs (Lichtenstein *et al.*, 1998; de Wit *et al.*, 1999). The cells were then warmed for 15 min to 37°C to allow delivery of the antibody-synaptotagmin complex to SLMVs. Although synaptotagmin is targeted from both the plasma membrane and EEs to SLMVs (Blagoveshchenskaya *et al.*, 1999), the antibody internalization method allowed us to selectively assay SLMV formation from EEs. Analysis of glycerol gradient fractions revealed a single peak of  $^{125}\text{I}$ -Cl 604.1 radioactivity in SLMV enriched fractions 8–10, which was not found in control assays carried out at 0°C (Figure 6). Clearly, SLMVs were most efficiently formed in the Q67Lrab4 transfectant (Figure 6), in which we observed a 2.5-fold increase in the amount of SLMVs compared with that in wild-type rab4 cells and nontransfected controls. The  $^{125}\text{I}$ -Cl 604.1 peak

around fractions 8–10 is not due to general vesiculation of endosomes because budding reactions with cells that had internalized transferrin at 15°C did not yield a peak of transferrin on this gradient (our unpublished results). Formation of SLMVs was inhibited in S22Nrab4 cells. Differences in budding efficiencies were not caused by alterations in the rate or extent of  $^{125}\text{I}$ -Cl 604.1 internalization because the amount of  $^{125}\text{I}$ -Cl 604.1 in the 15°C SLMV donor fractions was the same in the four cell lines (our unpublished results). In addition, subcellular fractionation of CHO- or Madin Darby canine kidney cells expressing the same rab4 constructs as the PC12 transfectants revealed that >80% of each of the three rab4 forms was associated with membranes (our unpublished results). It is quite unlikely therefore, that distinct distributions of the three rab proteins over membranes and cytosol of PC12 cells is causing the different budding efficiencies. These results corroborate our morphological findings that rab4 plays a direct role in SLMV formation from EEs.

#### Budding of EE-derived Vesicles Containing Tf-HRP Is Inhibited by S22Nrab4

We next assessed whether rab4 also regulates budding of Tf-containing vesicles in a cell-free system that generates vesicles from PC12 EEs (Clift-O'Grady *et al.*, 1998). Tf-HRP was accumulated in EEs during internalization at 15°C. The cells were then homogenized, and a postnuclear supernatant was prepared and used as donor membrane fraction in the assay. Donor fractions were next incubated with rat brain cytosol and ATP at either 0 or 37°C. After 30 min, budding reactions were resolved on sucrose gradients. Examination of Tf-HRP activity from a 0°C budding reaction revealed a peak of fast sedimenting endosomes at 38% sucrose and a peak of slower sedimenting endosomes at 24% sucrose (Figure 7A). During a 37°C budding reaction, Tf-HRP activity in the 24% endosome peak was reduced, with the concomitant appearance of a new peak at 20% sucrose (Figure 7A). We also tested whether inclusion of rat brain cytosol was essential to the efficiency of the budding reaction. As shown in Figure 7A, endogenous PC12 cytosol present in the donor membrane fraction was already sufficient to drive the budding reaction. Tf-HRP-containing vesicles that were formed during the assay sedimented at a position close to but distinct from the SLMV peak (our unpublished results). Little if any of the 38% sucrose endosome peak was affected. The position of the peaks in the gradient was the same for control PC12 cells and the cell lines transfected with rab4 constructs. Quantitation (normalized to the amount present in the respective donor fractions) of Tf-HRP activity in the 20% sucrose peaks, revealed similar budding-efficiency in reactions containing membranes prepared from wild-type rab4 cells and Q67Lrab4 cells. This contrasts with the result of the SLMV budding assay in rab4Q67L cells and may either reflect differences between the *in vivo* SLMV- and the *in vitro* Tf-HRP budding assays or suggest distinct molecular mechanisms that regulate SLMV and Tf-HRP vesicle formation. The formation of Tf-HRP vesicles was strikingly inhibited in S22Nrab4 cells as shown in Figure 7B. In five independent experiments, the amount of Tf-HRP in the 20% peaks at 37°C was reduced more than twofold in the S22Nrab4 cells (Figure 7C). Finally, the different cell lines contained the same amount of Tf-HRP at 15°C, ruling out the possibility that the lower budding effi-

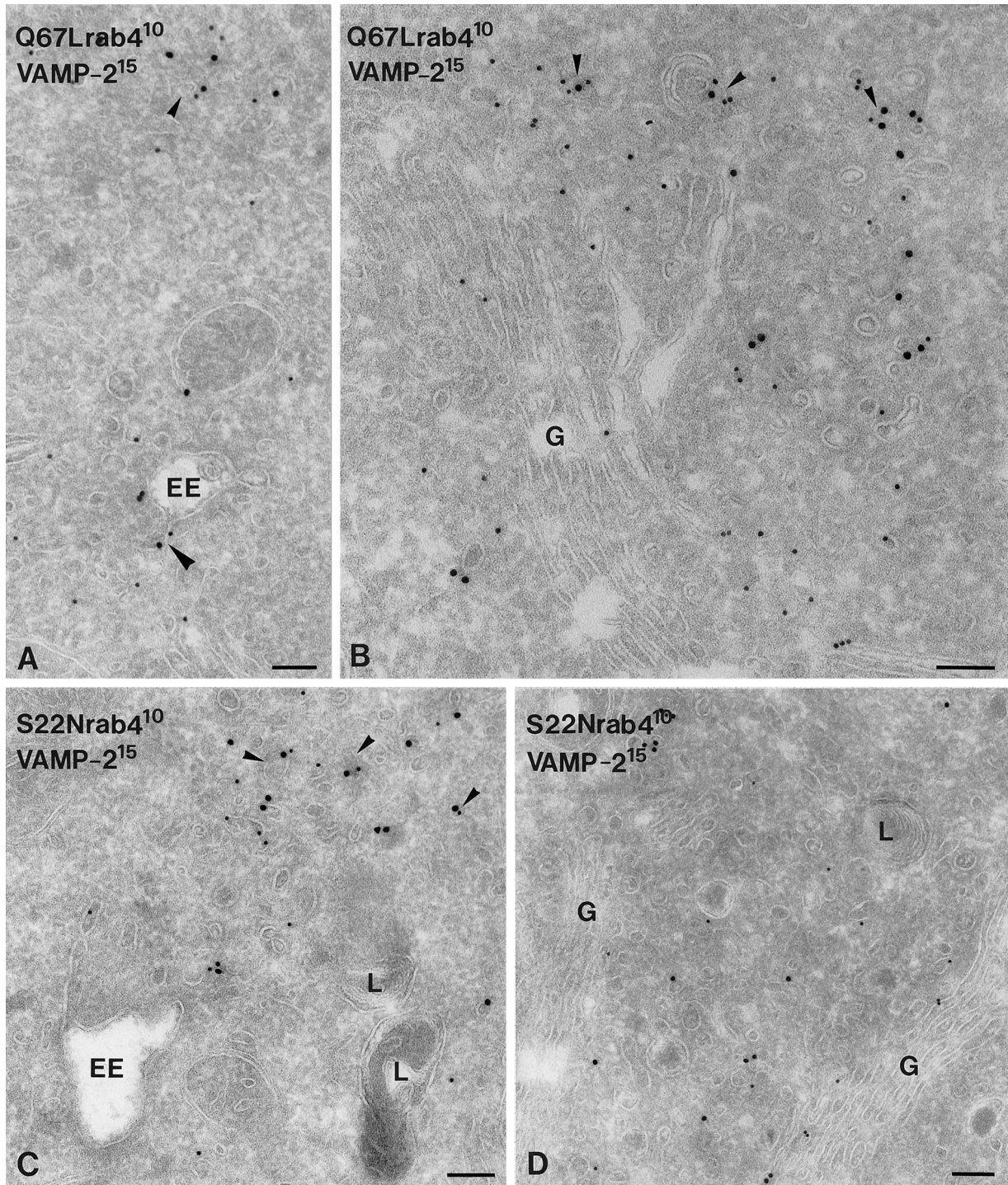


**Figure 3.** Ultrathin cryosections of rab4 mutant cells, double-immunogold labeled for VAMP2 (15 nm gold) and rab4 (10 nm gold). (A) VAMP2 and Q67Lrab4 colocalized in few EE-associated (large arrowhead) and cytoplasmic (small arrowhead) tubulo-vesicles. (B) Most vesicles harboring VAMP2 and Q67Lrab4 were found in the Golgi (G) area (arrowheads). (C) In S22Nrab4 cells, VAMP2 and rab4 colocalized on numerous EE-associated and nearby located tubules and vesicles (arrowheads). (D) Small vesicles in the Golgi area stained moderately for VAMP2 and S22Nrab4. L, lysosome. Bars, 100 nm.

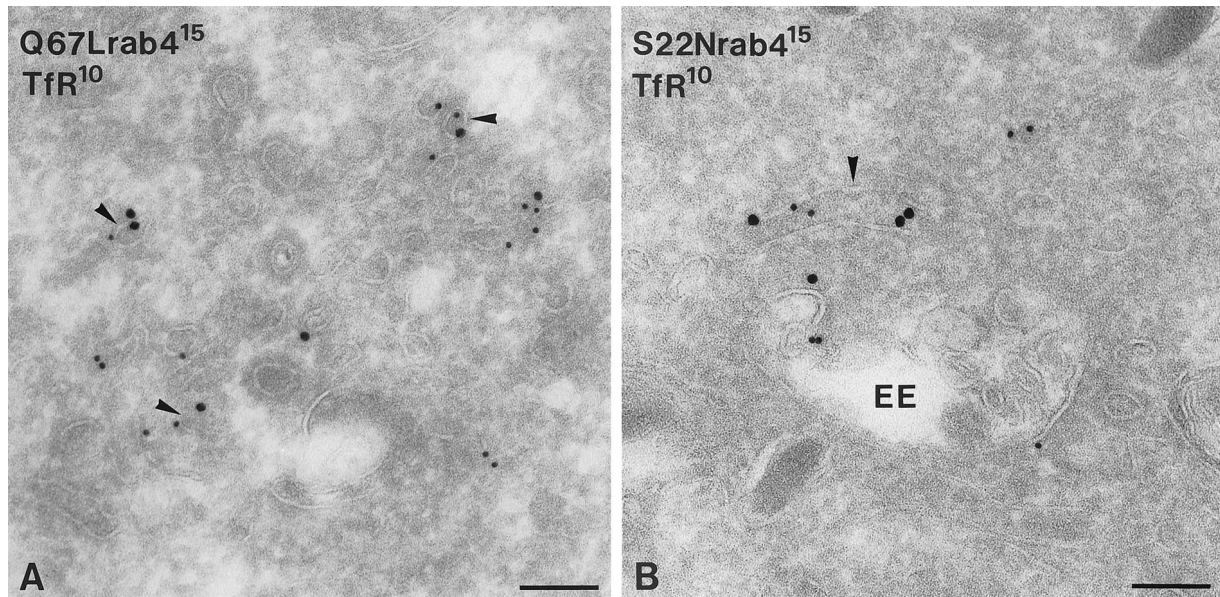


**Figure 4.** Cryosections of rab4 mutant cells double-immunogold labeled for rab4 (15 nm gold) and TfR (10 nm gold). (A) In Q67Lrab4 cells, TfR and rab4 localized to the same vesicles (arrowheads). (B) In S22Nrab4 cells, colocalization of rab4 and TfR was more frequently observed on EE-associated vesicles and tubules (arrowhead). Bars, 100 nm.

ciency in S22Nrab4 cells was caused by less efficient accumulation of Tf-HRP in these cells.

## DISCUSSION

Previously we provided the first ultrastructural characterization of the SLMV recycling pathway in neuroendocrine PC12

cells and showed that SLMV formation occurs from EEs (de Wit *et al.*, 1999). Because rab4 is predominantly localized to EEs and associated vesicles (de Wit *et al.*, 1999), we here investigated whether this small GTPase was of functional significance to SLMV formation. The main conclusion of our experiments is that rab4-GTP controls formation of SLMVs and of TfR-containing constitutive recycling vesicles from EEs. This con-

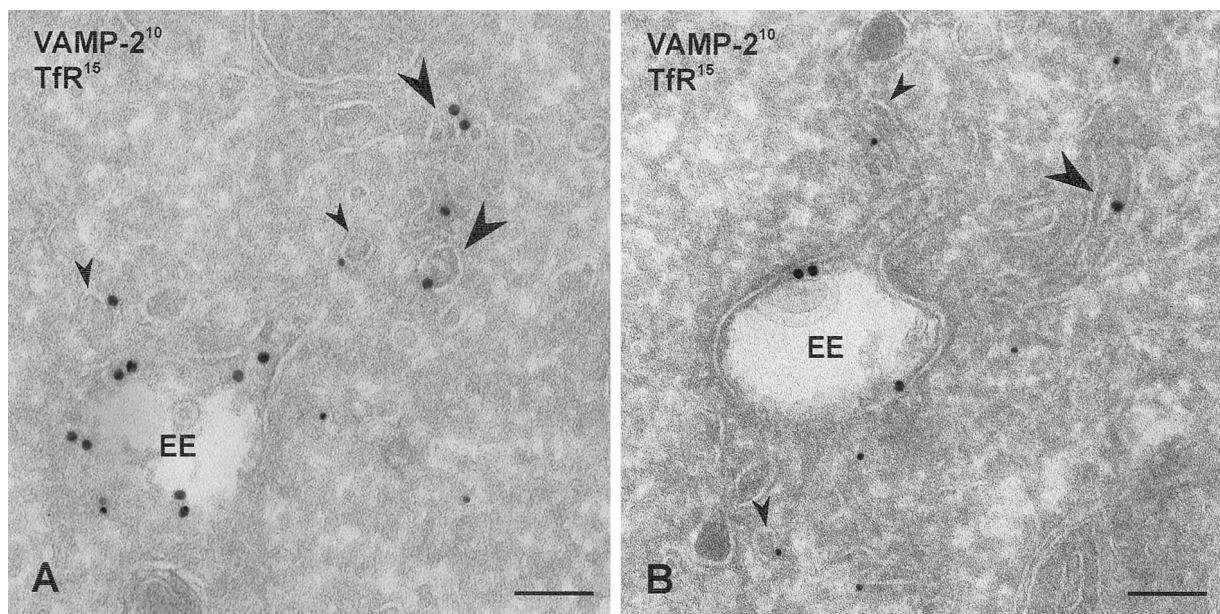


**Figure 5.** Cryosections of PC12 cells transfected with S22Nrab4 and double-immunogold labeled for VAMP2 (10 nm gold) and TfR (15 nm gold). (A) VAMP2 and TfR localized in EE vacuoles, but most EE-associated tubulovesicles contained either VAMP2 (large arrowheads) or TfR (small arrowheads). Bars, 100 nm.

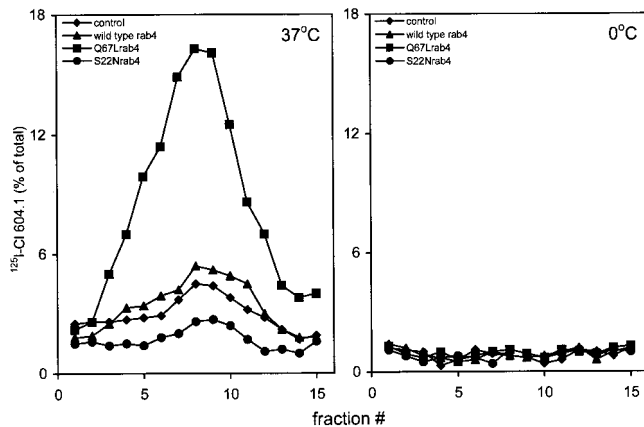


**Figure 6.** SLMV formation in PC12 cells expressing rab4, Q67Lrab4, and S22Nrab4. Cells were labeled with  $^{125}\text{I}$ -CI 604.1 mAb against synaptotagmin for 40 min at 15°C, washed, and reincubated with fresh medium for 15 min at 37°C or at 0°C. SLMVs were isolated on glycerol velocity gradients. A single peak of labeled SLMVs appeared in fraction 8–10 that is not affected in cells expressing rab4 ( $\blacktriangle$ ) as compared with control cells ( $\blacklozenge$ ). In contrast, SLMV formation was enhanced 2.5-fold in Q67Lrab4 cells ( $\blacksquare$ ) and inhibited in S22Nrab4 cells ( $\bullet$ ). Data represent the distribution of  $^{125}\text{I}$ -CI 604.1 in SLMVs as percentage of internalized antibody in the endosome donor, and are a representative of four independent experiments.

clusion is supported by several lines of evidence. First, cells expressing the GDP-binding mutant S22Nrab4 contained significantly extended EE tubules, whereas those expressing the GTPase-deficient mutant Q67Lrab4 had more EE-associated vesicles, suggesting that the GTP conformation of rab4 is required for vesicle formation. Second, the distribution of the rab4 mutants and of the marker proteins VAMP2 and TfR paralleled the morphological changes seen after ectopic expression of mutant forms of the GTPase. Finally, EE budding assays showed that Q67Lrab4 enhanced the formation of SLMVs, whereas S22Nrab4 inhibited budding of vesicles containing internalized iodinated synaptotagmin antibody or Tf-HRP. These results were derived from assays that measured VAMP2 and synaptotagmin, SLMV markers that might be targeted via distinct and overlapping pathways to SLMVs (Shi *et al.*, 1998; Blagoveshchenskaya *et al.*, 1999). This potential caveat, however, in no way affects the central conclusion of this article because we selectively quantitated SLMVs originating from EEs and not from the plasma membrane. In the EM studies this was done by counting labeled VAMP2 on or within 100 nm distance from EEs, whereas in the biochemical budding assays, we measured synaptotagmin with the use of an antibody that was preinternalized into EEs at 15°C.

Several exit routes are known for EEs. One of them leads to late endosomes/lysosomes and is not regulated by rab4 (van der Sluijs *et al.*, 1992). The other pathways are used for recycling from EEs to the cell surface. TfR is transported directly from EEs via a short circuit route to the plasma membrane and by a parallel pathway in which it is initially targeted to a perinuclear recycling endosome enriched in cellubrevin and rab11 before its delivery to the plasma membrane (Yamashiro *et al.*, 1984; Daro *et al.*, 1996; Ullrich *et al.*, 1996). In PC12 cells, SLMV proteins are sorted away from TfR in EEs and leave

them via yet another class of vesicles constituting a specialized recycling pathway from EEs (Lichtenstein *et al.*, 1998; de Wit *et al.*, 1999). Several studies have suggested a role for rab4 in transport from EEs to recycling endosomes (Sheff *et al.*, 1999; Sönnichsen *et al.*, 2000; van der Sluijs *et al.*, 1992). Our present study extends these data to neuroendocrine cells, but more importantly, adds a novel function for rab4 in the formation of SLMVs and transport vesicles from EEs.

The observations that a sizeable portion of Q67Lrab4 colocalized with VAMP2 and TfR in SLMVs and transport vesicles, respectively, and that neither wild-type rab4 nor Q67Lrab4 were found on the plasma membrane suggested that these rab4-positive vesicles are not targeted directly to the cell surface. Possibly, the VAMP2-containing vesicles, like the majority of the TfR vesicles, are first targeted to the perinuclear Golgi area before they evolve in mature SLMVs. Because rab3a is also associated with SLMVs and SVs and is known to act at a late stage of SV fusion with the plasma membrane (Geppert *et al.*, 1997), rab4 and rab3a sequentially might regulate transport of SV proteins through the EE system and to the cell surface. This hierarchical organization of rab protein activity may represent a general principle in the regulation of membrane transport. Indeed, the labs of Ullrich and Zerial recently showed that endocytosed Tf first colocalized with rab5/rab4 on EEs and subsequently with rab4/rab11 in recycling endosomes (Sönnichsen *et al.*, 2000; Trischler *et al.*, 1999). Whether rab4 is required for the recruitment of rab11 and rab3 remains to be established. A model describing the regulatory role of rab4 in distinct trafficking steps from early endosomes is shown in the schematic of Figure 8.

Rab4 did not appear to affect sorting of VAMP2 from TfR as we showed by double labeling for VAMP2 and TfR on cryosections of S22Nrab4 cells, suggesting that it acts distal to the primary sorting process of the two transmembrane proteins. The increased number of SLMVs and TfR-containing vesicles in Q67Lrab4 cells indicates that rab4 possibly exerts a specific effect on EE membrane domains that are involved in the formation of SLMVs and recycling vesicles. Such a function might include the formation of transport vesicles per se and the scission of tubulo-vesicular elements from EEs. In addition, it is formally possible that the increased number of SLMVs and recycling vesicles might be caused by an impaired ability of the vesicles to dock on their target organelle. Regardless whether rab4-GTP acts on the acceptor organelle as well, the immuno-EM clearly showed that expression of rab4 mutants induced differences of EE ultrastructure, consistent with a role of rab4 in vesicle budding. How then might rab4 regulate transport vesicle formation from EEs? Initially, rab proteins were perceived to act in docking/fusion of transport vesicles with target organelles (Bourne, 1988). It is clear now that small GTPases also play a key role in budding reactions (reviewed in Brittle and Waters, 2000; Der and Balch, 2000) and that the formation of a transport vesicle and its subsequent docking on a target organelle are mechanistically coupled. For instance, rab5 is a critical component in ligand sequestration into clathrin-coated pits at the plasma membrane (McLaughlan *et al.*, 1998) and the subsequent fusion of incoming uncoated vesicles with EEs (Bucci *et al.*, 1992). In the biosynthetic pathway, rab1-GTP is required for the formation of a complex containing the tethering protein p115 and the SNARE

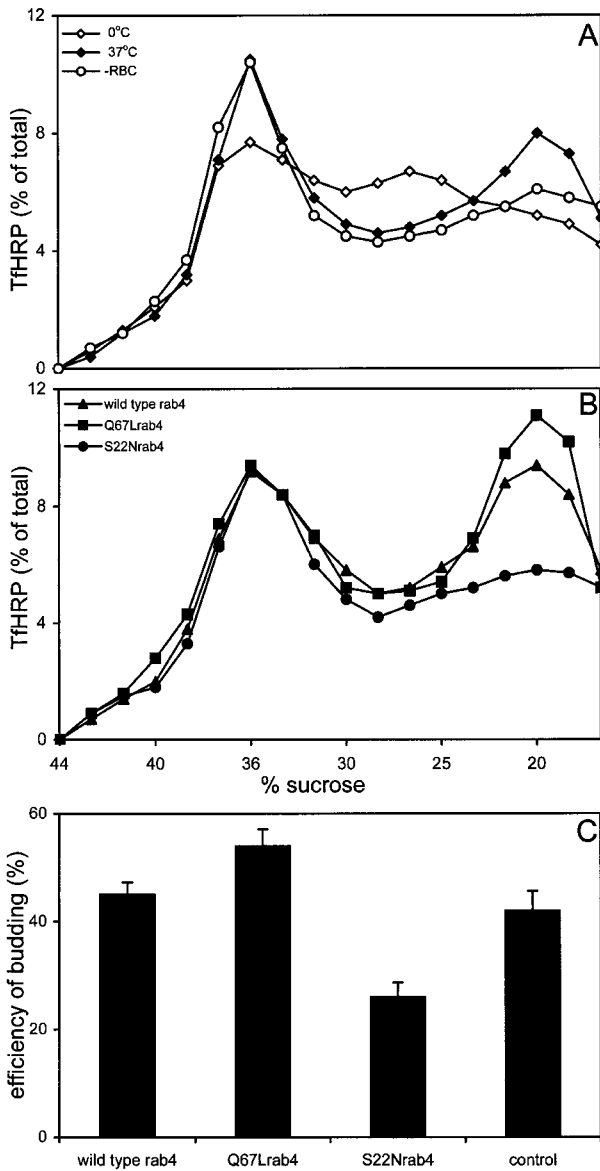


**Figure 7.** In vitro budding of Tf-HRP containing vesicles from EEs. Tf-HRP was internalized at 15°C in PC12 cells expressing rab4, Q67Lrab4, and S22Nrab4. After 40 min, the cells were washed and homogenized. (A) Donor fractions were prepared from nontransfected PC12 cells and incubated for 30 min with rat brain cytosol and ATP at 0°C (◇) and 37°C (◆) or in the absence of rat brain cytosol at 37°C (○). Budding reactions were resolved on sucrose gradients and Tf-HRP activity was analyzed colorimetrically. Tf-HRP activity in the 20% sucrose peak, represents the budding of vesicles produced from EEs at 37°C. (B) TfHRP vesicle budding-activity for donor membranes prepared from rab4 cells (▲), Q67Lrab4 cells (■), and S22Nrab4 cells (●) at 37°C. TfHRP activity in the gradient fractions is expressed as % of the conjugate internalized at 15°C and is a representative of 5 independent experiments. (C) Comparison of the 20% sucrose peaks formed at 37°C, revealed the same budding efficiency for donor membranes prepared from rab4 cells, Q67Lrab4 cells and control cells. In contrast, the formation of the Tf-containing transport vesicles in S22Nrab4 cells was inhibited twofold. Bars denote the average budding-efficiency of Tf-HRP containing transport vesicles recovered in the 20% peak fractions (±SEM, n = 5).

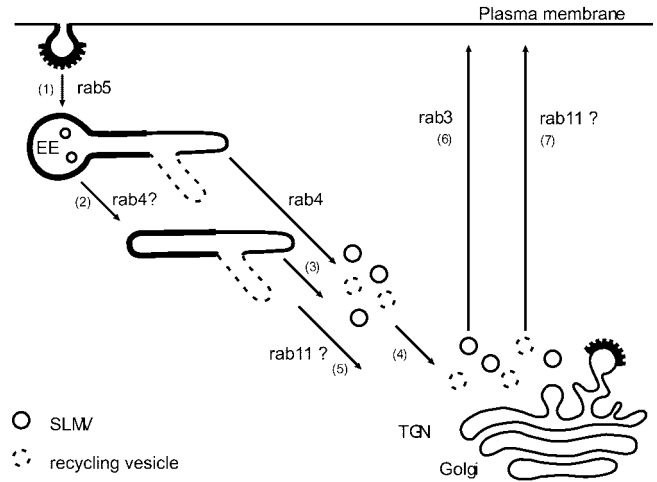


**Figure 8.** Model for the sequential action of rab proteins during the endosomal recycling pathway of SLMV-proteins and TfR in nondifferentiated PC12 cells. For reasons of clarity, we refrained from including the plasma membrane derived recycling pathway of SLMVs and the short circuit TfR recycling route. After rab5-dependent endocytosis in clathrin-coated vesicles, SLMV-proteins and TfR codistribute in EE vacuoles (1). Sorting of SLMV-proteins and TfR into distinct recycling tubules does not require the action of rab4 and may occur before or after (2) detachment of the tubules from the EE vacuole. SLMVs and recycling vesicles form through the action of rab4 (3), after which at least part of the newly formed vesicles translocates toward the Golgi area (4), via a pathway that possibly may depend on rab11 as well (5). Fusion of SLMVs with the plasma membrane requires rab3 (6), whereas transport of TfR containing vesicles to the plasma membrane is possibly regulated by rab11 (7).

proteins syntaxin5, membrin, and rbt1, which is essential for COPII-dependent transport between ER and Golgi complex (Allan *et al.*, 2000). We therefore propose that rab4 in its active form might recruit distinct effector and/or coat proteins to exit sites where vesicles of the regulated and constitutive recycling routes are formed. Because both the formation of SLMVs and of TfR recycling vesicles was controlled by rab4 (this study), different rab4 effectors could be used for vesicle formation in both pathways. Indeed, rabaptin5 binds to  $\gamma$ -adaptin (Hirst *et al.*, 2000), an AP-1 subunit that is present on EEs (Stoorvogel *et al.*, 1996; Futter *et al.*, 1998) and implicated in TfR recycling (Futter *et al.*, 1998). Because rab4 binds to the amino terminus of rabaptin4 and rabaptin5 (Vitale *et al.*, 1998; Nagelkerken *et al.*, 2000), it may locally regulate the activity of  $\gamma$ -adaptin. Interestingly, the ARF1 effector GGA2 (Boman *et al.*, 2000) also binds to rabaptin5 (Hirst *et al.*, 2000) and thereby might regulate ARF1-dependent SLMV formation from EEs (Faúndez *et al.*, 1997). The requirement of GGA2 in this process remains to be explored and future work will have to address which other proteins are present in these complexes and how they are assembled onto EEs. In a different scenario, rab4-GTP might interact with a putative microtubule motor protein that is recruited to the tubular extensions of EEs and could stimulate budding of transport vesicles, similar to models that have been proposed for rab5 (Nielsen *et al.*, 1999) and rab6 function (Echard *et al.*, 1998). Movement of this motor protein could then induce a pulling force to the tubular extensions and

contribute to vesiculation. This hypothesis is strengthened by the observation that nocodazole disperses transferrin and rab4-containing endosomes from the perinuclear region where the microtubule organization center is located, into the cytoplasm (Daro *et al.*, 1996). Although the precise molecular mechanism how rab4-GTP enhances formation of transport vesicles from EEs remains to be defined, several testable models have been derived that will allow to further elucidate the mechanisms regulating membrane recycling from EEs.

## ACKNOWLEDGMENTS

We are grateful to Reinhard Jahn (Max-Planck Institut für Biophysikalische Chemie, Göttingen, Germany) and Wieland Huttner (Department of Neurobiology, University of Heidelberg, Germany) for generously providing reagents. We thank Viola Oorschot and Richtje Leijendekker for technical assistance, Rene Scriwanek for preparation of the electron micrographs, and our colleagues in the Department of Cell Biology for their insightful comments. This work was supported by SLW grant 805-26-183 from the Life Sciences division of the Netherlands Organization of Scientific Research (to J.K. and P.v.d.S.) and National Institutes of Health grants NS09878 and DA10154 (to R.B.K.). Y.L. was supported by a postdoctoral fellowship of the Human Frontier Science Program.

## REFERENCES

- Allan, B.B., Moyer, B.D., and Balch, W.E. (2000). Rab1 recruitment of p115 into a cis-SNARE complex: programming budding COPII vesicles for fusion. *Science* 289, 444–448.
- Bauerfeind, R., Régner-Vigouroux, A., Flatmark, T., and Huttner, W. (1993). Selective storage of ACh, but not catecholamines, in neuroendocrine synaptic-like microvesicles of early endosomal origin. *Neuron* 11, 105–121.
- Blagoveshchenskaya, A.D., and Cutler, D.F. (2000). Sorting of synaptic-like microvesicles from early and late endosomes requires overlapping but not identical targeting signals. *Mol. Biol. Cell* 11, 1801–1814.
- Blagoveshchenskaya, A.D., Hewitt, E.W., and Cutler, D.F. (1999). Di-leucine signals mediate targeting of tyrosinase and synaptotagmin to synaptic-like microvesicles within PC12 cells. *Mol. Biol. Cell* 10, 3979–3990.
- Boman, A.L., Zhang, C.J., Zhu, X., and Kahn, R.A. (2000). A family of ADP-ribosylation factor effectors that can alter membrane transport through the *trans* Golgi. *Mol. Biol. Cell* 11, 1241–1255.
- Bottger, G., Nagelkerken, B., and van der Sluijs, P. (1996). Rab4 and rab7 define distinct endocytic compartments. *J. Biol. Chem.* 271, 29191–29197.
- Bourne, H.R. (1988). Do GTPases direct membrane traffic in secretion? *Cell* 53, 669–671.
- Brittle, E.E., and Waters, M.G. (2000). ER to Golgi traffic—this bud's for you. *Science* 289, 403–404.
- Bucci, C., Parton, R., Mather, I., Stunnenberg, H., Simons, K., and Zerial, M. (1992). The small GTPase rab5 functions as a regulatory factor in the early endocytic pathway. *Cell* 70, 715–728.
- Cameron, P.L., Südhof, T.C., Jahn, R., and De Camilli, P. (1991). Colocalization of synaptophysin with transferrin receptors: implication for synaptic vesicle biogenesis. *J. Cell Biol.* 114, 151–164.
- Chavrier, P., van der Sluijs, Z., Mishal, B., Nagelkerken, and Gorvel, J.P. (1997). Early endosome dynamics characterized by flow cytometry. *Cytometry* 29, 41–49.
- Clift-O'Grady, L., Desnos, C., Lichtenstein, Y., Faúndez, V., Horng, J.T., and Kelly, R.B. (1998). Reconstitution of synaptic vesicle biogenesis from PC12 cell membranes. *Methods* 16, 150–159.
- Clift-O'Grady, L., Linstedt, A., Lowe, A.W., Grote, E., and Kelly, R.B. (1990). Biogenesis of synaptic vesicle-like structures in a pheochromocytoma cell line. *J. Cell Biol.* 110, 1693–1703.
- Daro, E., van der Sluijs, P., Galli, T., and Mellman, I. (1996). Rab4 and cellubrevin define different early endosome populations on the pathway of transferrin receptor recycling. *Proc. Natl. Acad. Sci. USA* 93, 9559–9564.
- de Wit, H., Lichtenstein, Y., Geuze, H., Kelly, R.B., van der Sluijs, P., and Klumperman, J. (1999). Synaptic vesicles form by budding from tubular extensions of sorting endosomes in PC12 cells. *Mol. Biol. Cell* 10, 4163–4176.
- Der, C., and Balch, W.E. (2000). GTPase traffic control. *Nature* 405, 749–751.
- Desnos, C., Clift-O'Grady, L., and Kelly, R.B. (1995). Biogenesis of synaptic vesicles in vitro. *J. Cell Biol.* 130, 1041–1050.
- Echard, A., Jollivet, F., Martinez, O., Lacapere, J.J., Rousset, A., Janoueix-Lerosey, I., and Goud, B. (1998). Interaction of a Golgi associated kinesin-like protein with rab6. *Science* 279, 580–585.
- Edelmann, L., Hanson, P.L., Chapman, E.R., and Jahn, R. (1995). Synaptobrevin binding to synaptophysin: a potential mechanism for controlling the exocytic fusion machine. *EMBO J.* 14, 224–231.
- Faúndez, V., Horng, J.T., and Kelly, R.B. (1997). ADP ribosylation factor 1 is required for synaptic vesicle budding in PC12 cells. *J. Cell Biol.* 138, 505–515.
- Faúndez, V., Horng, J.T., and Kelly, R.B. (1998). A function for the AP3 coat complex in synaptic vesicle formation from endosomes. *Cell* 93, 423–432.
- Futter, C.E., Gibson, A., Allchin, E.H., Maxwell, S., Ruddock, L.J., Odorizzi, G., Domingo, D., Trowbridge, I.S., and Hopkins, C.R. (1998). In polarized MDCK cells basolateral vesicles arise from clathrin- $\gamma$  adaptin-coated domains on endosomal tubules. *J. Cell Biol.* 141, 611–624.
- Geppert, M., Goda, Y., Stevens, C.F., and Südhof, T.C. (1997). Rab3A regulates a late step in synaptic vesicle fusion. *Nature* 387, 810–814.
- Geuze, H.J., Slot, J.W., Strous, G.J., Peppard, J., von Figura, K., and Schwartz, A.L. (1984). Intracellular receptor sorting during endocytosis: comparative immunoelectron microscopy of multiple receptors in rat liver. *Cell* 37, 195–204.
- Gorvel, J.P., Chavrier, P., Zerial, M., and Gruenberg, J. (1991). Rab5 controls early endosome fusion in vitro. *Cell* 64, 915–925.
- Hannah, M.J., Schmidt, A.A., and Huttner, W.B. (1999). Synaptic vesicle biogenesis. *Annu. Rev. Cell Dev. Biol.* 15, 733–798.
- Hirst, J., Lui, W.W.Y., Bright, N.A., Totty, N., Seaman, M.N.J., and Robinson, M.S. (2000). A family of proteins with  $\gamma$ -adaptin and VHS domains that facilitate trafficking between the *trans* Golgi network and the vacuole/lysosome. *J. Cell Biol.* 149, 67–69.
- Klumperman, J., Hille, A., Veenendaal, T., Oorschot, V., Stoorvogel, W., von Figura, K., and Geuze, H.J. (1993). Differences in the endosomal distributions of the two mannose 6-phosphate receptors. *J. Cell Biol.* 121, 997–1010.
- Lichtenstein, Y., Desnos, C., Faúndez, V., Kelly, R.B., and Clift-O'Grady, L. (1998). Vesiculation and sorting from PC12-derived endosomes in vitro. *Proc. Natl. Acad. Sci. USA* 95, 11223–11228.
- Linstedt, A.D., and Kelly, R.B. (1991). Synaptophysin is sorted from endocytic markers in neuroendocrine PC12 cells but not transfected fibroblasts. *Neuron* 7, 309–317.

- Marsh, M., Griffith, G., Dean, G., Mellman, I., and Helenius, A. (1986). Three dimensional structure of endosomes in BHK-21 cells. *Proc. Natl. Acad. Sci. USA* 83, 2899–2903.
- McLaughlan, H., Newell, J., Morrice, N., Osborne, A., West, M., and Smythe, E. (1998). A novel role for rab-GDI in ligand sequestration into clathrin-coated pits. *Curr. Biol.* 8, 34–45.
- Nagelkerken, B., van Anken, E., van Raak, M., Gerez, L., Mohrmann, K., van Uden, N., Holthuizen, J., Pelkmans, L., and van der Sluijs, P. (2000). Rabaptin4, a novel effector of rab4a, is recruited to perinuclear recycling vesicles. *Biochem. J.* 346, 593–601.
- Nielsen, E., F. Severin, J.M. Backer, A.A. Hyman, and Zerial, M. (1999). Rab5 regulates motility of early endosomes on microtubules. *Nat. Cell Biol.* 1, 376–382.
- Owen, D.J., Vallis, Y., Noble, M.J.E.M., Hunter, J.B., Dafforn, T.R., Evans, P.R., and McMahon, H.T. (1999). A structural explanation for the binding of multiple ligands by the  $\alpha$ -adaptin appendage domain. *Cell* 97, 805–815.
- Page, L., Sowerby, P.J., Lui, W.W.Y., and Robinson, M.S. (1999).  $\gamma$ -synergin: an EH domain-containing protein that interacts with  $\gamma$ -adaptin. *J. Cell Biol.* 146, 993–1004.
- Schmidt, A., Hannah, M.J., and Huttner, W.B. (1997). Synaptic-like microvesicles of neuroendocrine cells originate from a novel compartment that is continuous with the plasma membrane and devoid of transferrin receptor. *J. Cell Biol.* 137, 445–458.
- Schmidt, A., Wolde, M., Thiele, C., Fest, W., Kratzin, H., Podtelejnikov, A.V., Witke, W., Huttner, W.B., and Söling, H.D. (1999). Endophilin I mediates synaptic vesicle formation by transfer of arachidonate to lysophosphatidic acid. *Nature* 401, 133–141.
- Sheff, D.R., Daro, E.A., Hull, M., and Mellman, I. (1999). The receptor recycling pathway contains two distinct populations of early endosomes with different sorting functions. *J. Cell Biol.* 145, 123–139.
- Shi, G., Faúndez, V., Roos, J., Dell'Angelica, E.C., and Kelly, R.B. (1998). Neuroendocrine synaptic vesicles are formed in vitro by both clathrin-dependent and clathrin-independent pathways. *J. Cell Biol.* 143, 947–955.
- Shibata, H., Omata, W., Suzuki, Y., Tanaka, S., and Kojima, I. (1996). A synthetic peptide corresponding to the rab4 hypervariable carboxyterminal domain inhibits insulin action on glucose transport in rat adipocytes. *J. Biol. Chem.* 271, 9704–9709.
- Slot, J.W., Geuze, H.J., Gigengack, S., James, D.E., and Lienhard, G.E. (1991). Translocation of the glucose transporter GLUT4 in cardiac myocytes of the rat. *Proc. Natl. Acad. Sci. USA* 88, 7815–7819.
- Sönnichsen, B., De Renzis, S., Nielsen, E., Rietdorf, J., and Zerial, M. (2000). Distinct membrane domains on endosomes in the recycling pathway visualized by multicolor imaging of rab4, rab5, and rab11. *J. Cell Biol.* 149, 901–913.
- Staubli, W., Hess, R., and Weibel, E.R. (1969). Correlated morphometric and biochemical studies on the liver cell. II. Effects of phenobarbital on rat hepatocytes. *J. Cell Biol.* 2(42), 92–112.
- Stoorvogel, W., Oorschot, V., and Geuze, H.J. (1996). A novel class of clathrin coated vesicles budding from endosomes. *J. Cell Biol.* 132, 21–34.
- Trischler, M., Stoorvogel, W., and Ullrich, O. (1999). Biochemical analysis of distinct rab5- and rab11 positive endosomes along the transferrin pathway. *J. Cell Sci.* 112, 4773–4783.
- Ullrich, O., Reinsch, O., Urbe, S., Zerial, M., and Parton, R. (1996). Rab11 regulates recycling through the pericentriolar recycling endosome. *J. Cell Biol.* 135, 913–924.
- van der Sluijs, P., Hull, M., Webster, P., Goud, B., and Mellman, I. (1992). The small GTP binding protein rab4 controls an early sorting event on the endocytic pathway. *Cell* 70, 729–740.
- Vitale, G., Rybin, V., Christoforidis, S., Thornqvist, P.O., McCaffrey, M., Stenmark, H., and Zerial, M. (1998). Distinct rab-binding domains mediate the interaction of rabaptin-5 with GTP-bound rab4 and rab5. *EMBO J.* 17, 1941–1951.
- Vollenweider, P., Martin, S.S., Haruta, T., Morris, A.J., Nelson, J.G., Cormont, M., Le Marchand Brustel, Y., Rose, D.W., and Olefsky, J.M. (1997). The small GTP binding protein rab4 is involved in insulin induced GLUT4 translocation and actin filament rearrangement in 3T3-L1 cells. *Endocrinology* 138, 4941–4949.
- Weibel, E.R., Strauble, W., Guagi, H.R., and Hess, F.A. (1969). Correlated morphometric and biochemical studies on the liver cell. I. Morphometric model, stereologic methods, and normal morphometric data for rat liver. *J. Cell Biol.* 42, 68–91.
- White, S., Miller, K., Hopkins, C., and Trowbridge, I.S. (1992). Monoclonal antibodies against defined epitopes of the human transferrin receptor cytoplasmic tail. *Biochim. Biophys. Acta* 1136, 28–34.
- Yamashiro, D.J., Tycko, B., Fluss, S.R., and Maxfield, F.R. (1984). Segregation of transferrin to a mildly acidic (pH 6.5) para-Golgi compartment in the recycling pathway. *Cell* 37, 789–800.
- Zahraoui, A., Touchot, N., Chardin, P., and Tavitian, A. (1989). The human rab genes encode a family of GTP-binding proteins related to yeast YPT1 and SEC4 products involved in secretion. *J. Biol. Chem.* 264, 12394–12401.